Structure of the Native Cysteine-Sulfenic Acid Redox Center of Enterococcal NADH Peroxidase Refined at 2.8 Å Resolution[†,‡]

Joanne I. Yeh,[§] Al Claiborne,[||] and Wim G. J. Hol*[,§]

Biomolecular Structure Center, Department of Biological Structure, Howard Hughes Medical Institute, Box 357742, University of Washington, Seattle, Washington 98195-7442, and Department of Biochemistry, Wake Forest University Medical Center, Winston-Salem, North Carolina 27157

Received May 1, 1996; Revised Manuscript Received June 17, 1996[⊗]

ABSTRACT: In order to obtain the crystal structure of the flavoprotein NADH peroxidase with its native Cys42-sulfenic acid redox center, a strategy combining reduced exposure of crystals to ambient oxygen and data collection at −160 °C was applied. The structure of the native enzyme to 2.8 Å resolution is described; these results conclusively establish the existence of the Cys42-sulfenic acid as the functional non-flavin redox center of the peroxidase and provide the first structure for any naturally occurring protein-sulfenic acid. The Cys42-sulfenic acid atoms Cα−Cβ−Sγ−O roughly define a planar arrangement which is stacked parallel to the *si* face of the FAD isoalloxazine and positions the sulfenyl oxygen atom only 3.3 Å from FAD-C4A. His10-Nϵ2 contributes a hydrogen bond to the sulfenic acid oxygen, at a distance of 3.2 Å. Although one oxygen atom (OX1) of the non-native Cys42-sulfonic acid derivative identified in the earlier wild-type peroxidase structure was taken to represent the native Cys42-sulfenic acid oxygen [Stehle, T., Ahmed, S. A., Claiborne, A., & Schulz, G. E. (1991) *J. Mol. Biol. 221*, 1325−1344], this structure shows that the sulfenic acid oxygen does not occupy this position, nor is it hydrogen-bonded to Cys42-N as was OX1. Comparison of the native Cys42-sulfenic acid structure with that of two-electron reduced glutathione reductase provides an insight into the sulfenic acid FAD charge-transfer interaction observed with both wild-type and His10 mutant peroxidases. A model of the E·NADH intermediate recently observed in stopped-flow analyses of the enzyme [Crane, E. J., III, Parsonage, D., Poole, L. B., & Claiborne, A. (1995) *Biochemistry 34*, 14114−14124] has also been generated to assist in analyzing the chemical mechanism of sulfenic acid reduction.

The flavoenzyme NADH peroxidase from *Enterococcus faecalis* 10C1 is a homotetrameric protein of 201 kDa which contains, in addition to FAD, a cysteinyl redox center which undergoes reversible two-electron reduction (to Cys-SH) and oxidation by H_2O_2 during the catalytic cycle (Claiborne et al., 1993, 1994). Results of a detailed chemical analysis (Poole & Claiborne, 1989a), which included metabolic labeling of the protein with [^{35}S]cysteine and FAB[1] -mass spectrometric analysis of an oxidized derivative of the active-site cysteinyl peptide, indicated that a sulfenic acid derivative of Cys42 (Cys42-SOH) served as the non-flavin redox center. However, the X-ray crystal structure of the wild-type peroxidase refined at 2.16 Å resolution (Stehle et al., 1991) revealed that Cys42 had been oxidized to the sulfonic acid (Cys42-SO_3H). This result was attributed to the long periods during which protein crystals were exposed to atmospheric oxygen prior to data collection. The structures of both the free Cys42-SO_3H form of the peroxidase and its NADH complex (Stehle et al., 1993) demonstrated that one of the sulfonic acid oxygens (OX1) was hydrogen-bonded both to the His10 imidazole and to the Cys42 backbone amide nitrogen; on this basis, Stehle et al. (1991, 1993) concluded that OX1 corresponds to the sulfenic acid oxygen of the native peroxidase. Additionally, treatment of the native enzyme with millimolar concentrations of H_2O_2 led to inactivation of the cysteinyl redox center and irreversible loss of peroxidase activity (Poole & Claiborne, 1989a); these results were attributed to oxidation of the cysteine-sulfenic acid (Cys42-SOH) to cysteine-sulfinic (Cys42-SO_2H) and/or -sulfonic acid (Cys42-SO_3H) forms similar to that observed in the crystal structures.

Recent studies continue to substantiate the proposal that the non-flavin redox center is indeed Cys42-SOH. C42S and C42A mutants lacking this residue (Cys42 is the only cysteine in the protein) have very low activity levels, approximately 0.04% of that of the wild-type enzyme (Parsonage & Claiborne, 1995); flavin reduction by NADH is very rapid, but the $FADH_2$ enzyme is seriously impaired in its ability to catalytically reduce H_2O_2 without the essential reduced Cys42-thiolate. The refined 2.0 Å structures of both mutant proteins (Mande et al., 1995) confirm that other unanticipated conformational and/or structural changes have not accompanied replacement of Cys42 with Ser or Ala. In a separate study, four active-site mutants were generated in which each protein contained one new Cys in addition to Cys42−SOH (Miller et al., 1995); the L40C mutation led

[†] W.G.J.H. acknowledges the support of the Murdock Charitable Trust. A.C. acknowledges the support of National Institutes of Health Grant GM-35394.

[‡] Coordinates have been deposited in the Brookhaven Protein Data Bank under the file name 1JOA.

* To whom correspondence should be addressed.

[§] University of Washington.

[||] Wake Forest University Medical Center.

[⊗] Abstract published in *Advance ACS Abstracts,* July 15, 1996.

[1] Abbreviations: FAB, fast atom bombardment; Cys42-SOH, Cys42-sulfenic acid; Cys42-SO_3H, Cys42-sulfonic acid derivative of NADH peroxidase; BPV-1, bovine papillomavirus type 1; E, oxidized enzyme; EH_2, two-electron-reduced enzyme; GR, glutathione reductase; NPX, NADH peroxidase; WT, wild-type.

S0006-2960(96)01037-9 CCC: $12.00

Table 1: X-ray Data Collection and Final Refinement Statistics[a]

parameter	SOH	SO_3H
resolution range (Å)	50−2.8	50−2.5
resolution range used in refinement (Å)	8−2.8	8−2.5
total number of reflections	534847	248250
number of independent reflections	28235	62240
completeness in total (%)	100	85.1
completeness at highest resolution shell (%)	(2.93−2.80 Å) 99.9	(2.61−2.50 Å) 55.7
average temperature factor (all atoms) (Å^2)	20.7	19.3
unique reflections greater than 3σ	23331	53980
R_{merge}[b] (intensities) (%)	8.9	8.8
$R_{working}$[c] (%)	17.9	19.6
R_{free}[c] (%)	25.0	24.6
rms bond length (Å)	0.011	0.010
rms bond angle (deg)	2.9	2.7
number of protein atoms (including one FAD molecule)	3544	3544
number of non-protein atoms	185	−

[a] The SOH data set was collected on freshly grown crystals on an R-axis II system at −160 °C. The SO_3H data set was collected at Brookhaven National Laboratory at −160 °C on crystals stored at room temperature under ambient atmospheric conditions for approximately 7 months (see text). [b] $R = [\sum_{hkl}|I(hkl)-\langle I(hkl)\rangle|/\sum_{hkl}I(hkl)]\times 100$, where I is the intensity of the reflection. [c] $R = [\sum_{hkl}||F_o(hkl)|-|F_c(hkl)||/\sum|F_o(hkl)|]\times 100$, where F_o and F_c are the observed and calculated structure factor amplitudes, respectively, for the reflection.

to spontaneous Cys40-Cys42 disulfide formation. The refined 2.1 Å structure of this protein confirmed the presence of the new disulfide and, in combination with characterizations of the spectroscopic, catalytic, and redox properties of the L40C mutant, provided further indirect support for the identity of Cys42-SOH as the non-flavin redox center in the wild-type enzyme.

The presence of a cysteine-sulfenic acid moiety in a protein is intriguing in that there are few biochemical or chemical examples of naturally occurring or stable sulfenic acids. A recent structural example of a cysteine-sulfenic acid is the unexpectedly stable 4,6-dimethoxy-1,3,5-triazine-2-sulfenic acid, determined at 90 K (Tripolt et al., 1993). Sulfenic acids are generally prone to further oxidation to the sulfinic and sulfonic acid forms. These facile oxidation reactions have prevented detailed structural analysis of the active site of the peroxidase, and there is little detailed structural information available on the stabilization of sulfenic acid derivatives by elements of protein structures in general. This moiety may represent a novel class of redox-active centers, and it has been demonstrated that the enterococcal NADH oxidase ($2NADH + O_2 \rightarrow 2NAD^+ + 2H_2O$; Claiborne et al., 1993, 1994) is a homolog of the peroxidase. In the oxidase, Cys42 is conserved, and a Cys42-SOH structure has been proposed for the non-flavin redox center of this enzyme as well. Cys-SOH derivatives have also been proposed to play essential roles in the redox regulation of transcription factors such as Fos and Jun (Abate et al., 1990), OxyR (Storz et al., 1990; Kullik et al., 1995), bovine papillomavirus type 1 (BPV-1) E2 protein (McBride et al., 1992), and nuclear factor I (Bandyopadhyay & Gronostajski, 1994).

EXPERIMENTAL PROCEDURES

Protein Expression and Purification. The cloning, expression, and purification of the NPX have been described elsewhere (Ross & Claiborne, 1991; Parsonage et al., 1993). Briefly, NPX is expressed in *Escherichia coli* cells, JM109DE3, on induction with IPTG and harvested approximately 4 h after induction. Cells are harvested and washed with 50 mM phosphate buffer (pH 7.0) with 0.6 mM EDTA and then frozen at −80 °C. After the cells were broken and fractionation involving ammonium sulfate, the protein is purified to homogeneity with a combination of phenyl-Sepharose and Q-Sepharose column chromotography steps.

Crystallization. Crystals of the NADH peroxidase with the SOH moiety were obtained by the vapor-diffusion technique (Kim et al., 1973). In order to maintain the Cys42-SOH form, the crystals were freshly grown, thereby limiting aging (exposure) time to ambient atmospheric oxygen. Typically, time from crystallization to data collection was between 2 weeks and 2 months. In addition, a peroxidase assay on dissolved crystals was used to monitor and ascertain that the protein crystallized was indeed active. The new crystals were grown in the presence of cryoprotectants so that the crystals could be flash-frozen, which would additionally limit oxidation during data collection of the active-site Cys42-SOH to the inactive Cys42-SO_3H form, as originally observed by Stehle et al. (1991).

Crystals were grown from a solution containing 50% PEG 200 as both the precipitating agent and cryoprotectant and 100 mM Tris-HCl buffer (pH 7). The most optimum crystallization condition was established after observing that crystals grown in the presence of a small amount of glycerol had improved size and morphology compared to crystals obtained in the absence of glycerol. Glycerol was added to the protein stock solution to a final concentration of 10% glycerol. The final protein concentration was 8 mg/mL in 10 mM Tris-HCl buffer (pH 7). The largest crystals were grown from hanging drops, where the protein stock was diluted 1:1 with the crystallization solution and the final volume of the drop was 6 μL. Large, yellow, prism-shaped crystals appeared after approximately 30 h at 20 °C and continued to grow for about 10 days. The dimensions of the largest crystals were approximately 0.8 mm × 0.8 mm × 0.6 mm. The protein crystallized from the above solution in space group $I4_122$ with cell dimensions $a = b = 153.7$ Å and $c = 190.0$ Å, with one monomer per asymmetric unit. These crystals are entirely different from those obtained previously (Stehle et al., 1991; Mande et al., 1995; Miller et al., 1995). Data were collected at −160 °C after the crystal was flash-frozen in a nitrogen stream. Data were collected on an R-axis II system with an MSC cryo-cooling device and processed with Denzo (Otwinowski, 1993) when the

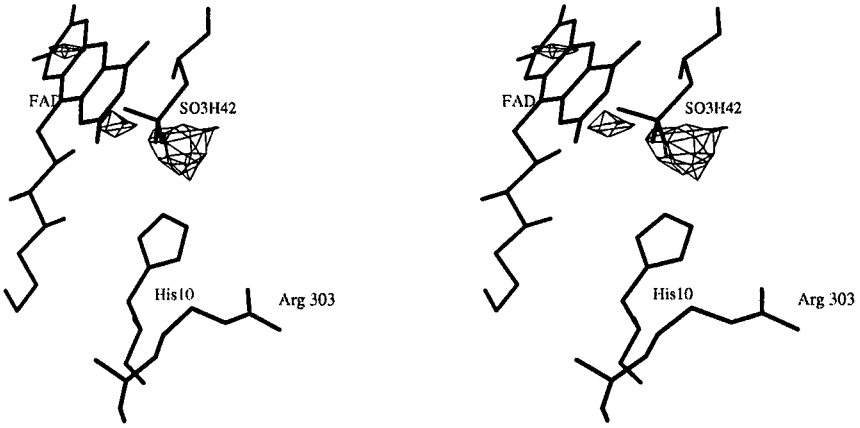

FIGURE 1: Electron density contoured at -2.5σ of the difference ($F_o - F_c$) σ_A weighted map, modeled with a cysteine-sulfonic acid (Cys42-SO_3H) at the active site. The resulting negative peaks at two of the three oxygens indicate that the model contains extraneous atoms at the active site.

R-axis software failed to index the crystal. Data collection statistics are reported in Table 1.

Crystallography and Structure Determination. The wild-type NPX coordinates were used as the starting model for the molecular replacement solution of the native, Cys42-SOH data set (hereon referred to as the "cryo data set" and "cryo crystals"). WT NPX originally crystallized in space group *I*222, with cell parameters $a = 77.2$ Å, $b = 134.5$ Å, and $c = 145.9$ Å (Stehle et al., 1991). The rotation and translation searches for the cryo data set were done in AMoRe (Navaza, 1994), and the model was refined in X-PLOR 3.0 (Brünger, 1992). The initial rotation search model included all residues, with residue 42 changed to a cysteine. This yielded an unambiguous rotation search solution that had a top solution with a correlation coefficient of 0.21 and a peak height of 12.4σ, with the next peak only 4.2σ. The Eulerian angles for this solution were 44.6, 90.5, and 91.1°. A translation search with these rotation angles yielded a solution with a correlation coefficient of 0.69 and a peak height of 29.7σ, with an *R* factor of 33.4%. The translation solution coordinates were 0.37, 0.4, and 0.4, in fractional coordinates. A cycle of rigid-body refinement in AMoRe increased the correlation coefficient to 0.7 and dropped the *R*-factor to 32.2%. This solution was refined in X-PLOR, where the reflections were randomly divided into two sets: a working set composed of approximately 90% of the reflections sampled at random and a test set composed of the remaining 10%, which was used for cross-validation of the refinement cycles. The weight used for the refinement was calculated through the "check" program in X-PLOR, and the value used was 50% of the calculated value, which was incrementally increased as refinement progressed. The initial refinement cycle started with conventional conjugate-gradient type minimization followed by molecular dynamics, simulated annealing, and temperature factor refinement. Electron density maps were calculated, and both σ_A weighted (Read, 1986) and unweighted maps were analyzed; both equivalently showed characteristic features at the active site. After each round of refinement, the model was inspected with both $(2F_o - F_c) \exp i\alpha_{cal}$ and $(F_o - F_c) \exp i\alpha_{cal}$ maps. Waters were built into the maps after the R-factor reached 22%. Each of the top 25−40 peaks in the difference map of each cycle was interpreted as a water position and was visually checked on the graphics system in order to determine whether it satisfied reasonable distances and geometry criteria necessary for assignment as a protein-associated water. The model currently contains 185 waters, 447 protein residues, and a FAD cofactor.

RESULTS

In order to ascertain that the Cys42-SOH had not been oxidized to the sulfinic Cys42-SO_2H or sulfonic Cys42-SO_3H acids, refinements were done with several models which differed at residue 42. These models included cysteine, alanine, Cys42-SOH, and Cys42-SO_3H at position 42. Omit difference maps, calculated after simulated annealing to reduce model bias, were then used to ascertain the amount of electron density that was present after omitting a specific region from the model. Refined omit maps were calculated by omitting from the model a region of 8 Å around a residue and refining the remaining model. Atoms within a 3 Å shell were restrained in order to avoid artificial movement into the omitted region. These maps show that the resulting difference electron density at position 42 best fits a Cys42-SOH model, whereas a Cys42-SO_3H results in negative density in the maps, indicating that the model contains too many atoms at that site (Figure 1).

A final check of the correctness of the Cys42-SOH center is the reproduction of the Cys42-SO_3H form under cryo conditions using "aged" crystals. Crystals, which had been grown about 7 months prior to data collection and stored at room temperature under ambient atmospheric conditions, were irradiated, and these data were processed as described above. This data set was collected at the Brookhaven National Laboratory on beamline X-12B at −160 °C; data collection statistics are reported in Table 1. This data set resulted in the triply oxidized Cys42-SO_3H form even though cryo conditions were also used (Figure 2). It is believed that exposure to ambient atmospheric oxygen prior to data collection causes this oxidation and that, in order to obtain the native, active-site Cys42-SOH moiety, both freshly grown crystals and cryo conditions are necessary to limit the extent of oxidation. Comparison of the Cys42-SOH structure to those known to contain a sulfonic acid center shows that the center in the native protein is unambiguously a Cys42-SOH (Figure 3).

The catalytic center consists of the isoalloxazine moiety of FAD, the sulfenic acid moiety of Cys42, and His10. The Cα−Cβ−S−O atoms of Cys42-SOH roughly define a

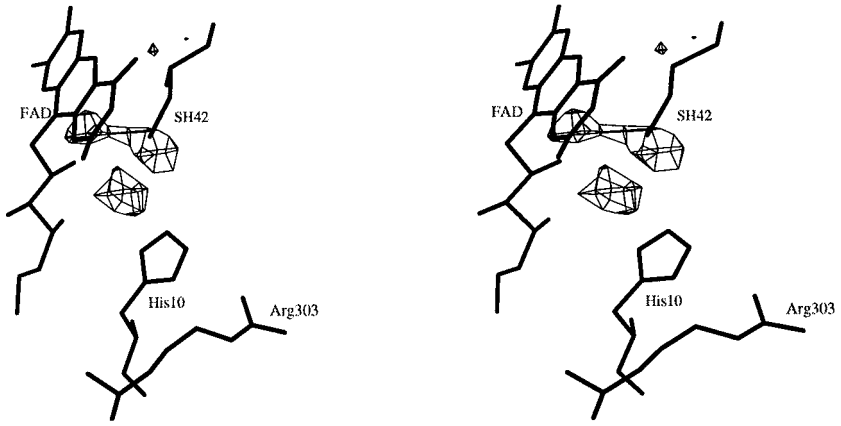

FIGURE 2: Electron density contoured at $+2.5\sigma$ of the difference $(F_o - F_c)$ σ_A weighted map, modeled with a cysteine at position 42 (Cys42-SH). This results in three distinct positive densities, showing that the presence of a sulfonic acid is unambiguous. The map was calculated from data collected on the overoxidized NPX crystals (see text). This was used as a comparison in identifying the sulfenic acid at position 42 of the cryo data set.

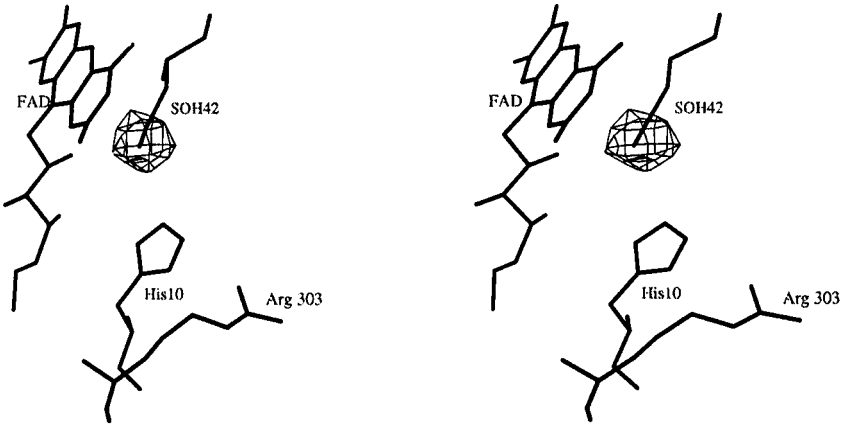

FIGURE 3: Electron density contoured at $+2.5\sigma$ of the difference $(F_o - F_c)$ σ_A weighted map, modeled with a cysteine at position 42 (Cys42-SH). This results in a single, large positive density at the oxygen position of the cysteine-sulfenic acid (Cys42-SOH). The figure is shown with a Cys-SOH at the active site to indicate the position of the redox-active group.

"plane" which stacks in parallel to the *si* face of the isoalloxazine ring, and the sulfenic acid oxygen occupies a position somewhat different from any of the three oxygens of the sulfonic acid center previously described and is most closely approximated by OX3 (Figure 4). It had been suggested that the sulfenic acid oxygen would occupy the position corresponding to the OX1 position of the sulfonic acid (Stehle et al., 1993). In this native structure, the Cys42-SOH oxygen occupies a position that optimizes interactions with the isoalloxazine ring of FAD and with His10, forming a geometrical arrangement that favors the charge-transfer interaction (Cys42-SOH → FAD) described previously for oxidized NPX.

Quality of the Final Model. The current model has an R_{free} of 25% and and $R_{working}$ of 17.9%. The rms for bond lengths is 0.011 Å and for bond angles is 2.9°. The mean coordinate error estimated from a σ_A plot (Read, 1986) is 0.15 Å. The Ramachandran plot of the current model which contains 394 non-glycine and non-proline residues shows that there are 342 residues in the most favored region (86.8%), and 49 more residues (12.4%) in additional allowed regions, as analyzed by PROCHECK (Lawkowski et al., 1992). There are two residues in the generously allowed regions, Asp291 (ϕ of 41°, ψ of 63°) and Met269 (ϕ of 57°, ψ of 10°), and a single residue, Phe332 (ϕ of 49°, ψ of −116°), in the disallowed region. Phe332 was seen previously to be an outlier (Stehle et al., 1991). This is due to Phe332 occupying position $i+1$ of a type II′ turn, where glycine is usually required.

DISCUSSION

The structure of the native Cys42-SOH redox center in the enterococcal NADH peroxidase is significant in several respects. Since Cys-SOH is generally unstable (Kice, 1980; Hogg, 1990), this structure allows us to interpret those elements of the peroxidase active site which are involved in Cys-SOH stabilization. Additionally, it has been demonstrated that reduction of the Cys42-SOH center, which involves hydride transfer from bound NADH in the conversion of E·NADH to EH_2, is rate-limiting in turnover (Crane et al., 1995); the structure of the native oxidized enzyme provides the basis for probing the chemical mechanism of Cys42-SOH reduction. The structural and mechanistic homology between NADH peroxidase and the flavoprotein NADH oxidase, which also contains a non-flavin redox center identified as Cys-SOH (Claiborne et al., 1993, 1994), indicates that these conclusions regarding Cys42-SOH stabilization and function will have a strong impact on studies of NADH oxidase structure and mechanism. And finally, Cys-SOH centers have been proposed to account for the redox regulation of the transcription factors Fos and Jun (Abate et al., 1990), OxyR (Storz et al., 1990; Kullik et al., 1995), BPV-1 E2 protein (McBride et al., 1992), and nuclear factor I (Bandyopadhyay & Gronostajski, 1994); the Cys42-

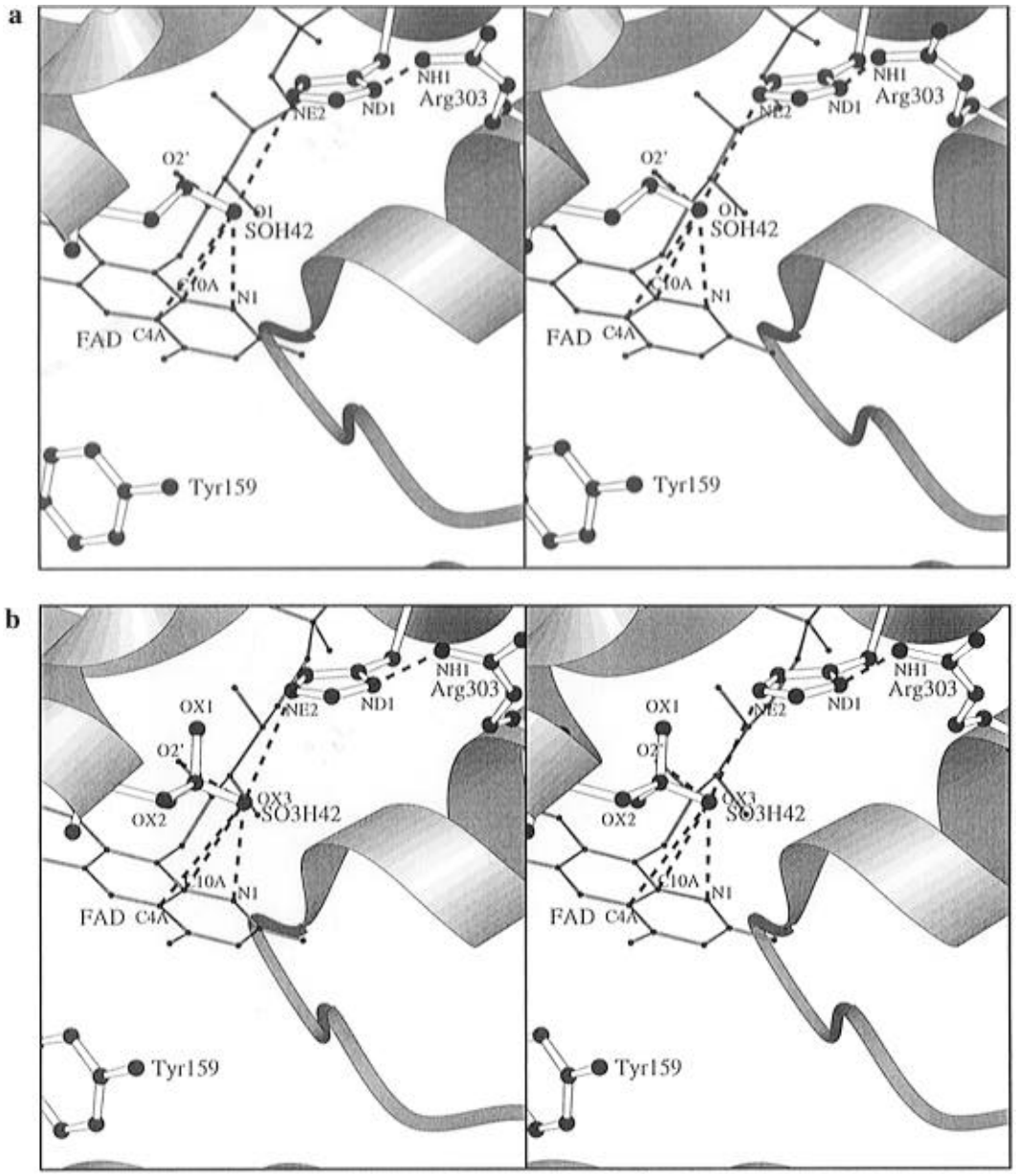

FIGURE 4: Comparison of the active site of the Cys42-SOH with the Cys42-SO_3H. The sulfenic acid oxygen occupies a position that optimizes the simultaneous interaction of this redox-active group with FAD and His10 (panel a). It was previously thought that the sulfenic acid oxygen would occupy the position of OX1 of the sulfonic acid structure. When the Cys42-SOH active site (panel a) is compared with the Cys42-SO_3H active site (panel b), OX3 is closest to the position of the redox-active sulfenic acid oxygen. The dotted lines indicate hydrogen-bonding partners (see text).

SOH structure described in this report provides a basis for further structural and functional tests of these models.

Four criteria developed for stabilization of Cys-SOH either in solution (Kice, 1980; Hogg, 1990) or in protein structures (Liu, 1977; Allison, 1976; Claiborne et al., 1993) are (1) intramolecular hydrogen bonding, (2) ionization to the conjugate sulfenate base, (3) the absence of other vicinal protein thiols, and (4) limited solvent accessibility and association with apolar elements of protein structure. The limited solvent accessibility and apolar microenvironment of Cys42 have been described previously (Claiborne et al., 1993), and Cys42 is the only cysteine residue in the peroxidase (Poole & Claiborne, 1988; Ross & Claiborne, 1991). This work establishes conclusively that His10-Nϵ2 is hydrogen bonded to the Cys42-SOH oxygen, at a distance of 3.2 Å. Furthermore, the environment of His10 clearly indicates that this residue serves as a hydrogen-bond donor, consistent with ionization of the Cys42-SOH. Since His10-Nδ1 is hydrogen-bonded to Arg303-NH2 at a distance of 2.9 Å, it must not be protonated. The second histidyl nitrogen, Nϵ2, should have a pK_a near 15 and therefore is most probably protonated. Crane et al. (1996) have recently shown that replacement of His10 with Gln, despite the fact that Gln also has an Nϵ atom, leads to a 50-fold increase in the second-order rate constant for H_2O_2 inactivation (via Cys42-SOH oxidation). This corresponds to a 2.3 kcal/mol destabilization of the ground state Cys42-SOH due to the absence of the His10-Nϵ2 hydrogen bond.

There are several active-site interactions indicated for the Cys42-SOH oxygen, and one of these involves a charge transfer with the electron-deficient isoalloxazine ring of FAD. The Cys42-SOH oxygen approaches within 3.2 Å of FAD-C10A, 3.3 Å of FAD-N1, and 3.3 Å of FAD-C4A; the corresponding distances for the Cys42-Sγ are 3.6, 4.1, and

3.7 Å. Additionally, the Cys42-SOH oxygen is in the vicinity of the FAD-O2′F at a distance of 3.5 Å. The presence of a very low-extinction, long-wavelength absorbance band extending to 700 nm has been noted repeatedly with preparations of wild-type peroxidase (Poole & Claiborne, 1986). This spectral feature was eventually attributed to an interaction between the anionic sulfenate form of Cys42-SOH and the oxidized flavin (Poole & Claiborne, 1989a). The high polarity of the sulfur−oxygen bond (Liu, 1977) was taken in support of the possibility that the electron-rich sulfenate oxygen could serve as a charge-transfer donor. The two crystal structures most relevant to this analysis are those of the two-electron-reduced glutathione reductase (complex with NADH; Karplus & Schulz, 1989) and the old yellow enzyme complex with *p*-hydroxybenzaldehyde (Fox & Karplus, 1994; Karplus et al., 1995). In the GR EH_2 form, the nascent Cys63-SH is stabilized as the thiolate (pK_a = 4.8 for the yeast enzyme; Williams, 1992) and serves as charge-transfer donor to the FAD isoalloxazine. When the active site of the NADH peroxidase is compared to that of the reduced glutathione reductase, a superposition of the respective FADS brings the Cys63-Sγ and the Cys42-SOH oxygen to nearly the same point without superposition of the protein residues themselves and may signify a general geometric arrangement for efficient redox activity. For the GR EH2 form, hydrogen bonds from Thr339-Oγ and FAD-O2′ and the charge-transfer interaction with FAD-C4A is well-oriented to stabilize the thiolate at favorable distances of 3.2, 3.4, and 3.3 Å, respectively (Karplus & Schulz, 1989). With old yellow enzyme, binding of *p*-hydroxybenzaldehyde gives rise to a long-wavelength absorbance band due to the charge-transfer interaction between the bound phenolate anion and oxidized FMN; the X-ray structure shows that the phenol ring is stacked parallel to the *si* face of the isoalloxazine, and the phenolate oxygen approaches within 3.0 Å of the FMN-C2. Binding of some phenolic ligands is accompanied by a dramatic decrease of 4 units in the phenolic pK_a, and the structure of the *p*-hydroxybenzaldehyde complex shows that, in addition to the charge-transfer interaction, hydrogen bonds from the neutral His191-Nϵ2 and Asn194-Nδ1 stabilize the phenolate anion. From these comparisons, we suggest that Cys42-SOH is stabilized in the peroxidase as the sulfenate anion through its charge-transfer interaction with FAD and its hydrogen bonds with His10-Nϵ2 and possibly with FAD ribityl O2′. However, the His10 mutants of NADH peroxidase also show enhanced charge-transfer absorbance bands in their Cys42-SOH forms (Crane et al., 1996). The pK_a of Cys42-SOH in the H10Q peroxidase is ≤4.5, based on a spectral pH titration.

Reduction of the wild-type peroxidase (EH_2) consists (Crane et al., 1995) of rapid binding of NADH to give the spectrally distinct E·NADH complex and a rate-limiting (25 s^{-1} at pH 7.0, 5 °C) intramolecular hydride transfer which yields EH_2 (+ NAD^+ + H_2O). Intermediate flavin reduction is not observed, and the chemical mechanism for Cys42-SOH reduction is not known. When the bound NADH from the wild-type Cys42-SO_3H peroxidase complex (Stehle et al., 1993) is modeled into the native structure, three largely parallel, stacked planes appear to correspond to the nicotinamide ring of NADH, the isoalloxazine moiety, and the plane roughly defined by Cys42-SOH (Cα−Cβ−Sγ−O). In the model, NADH binds at the flavin *re* face, and the nicotinamide C4N is 2.9 Å from FAD-N5F, the expected

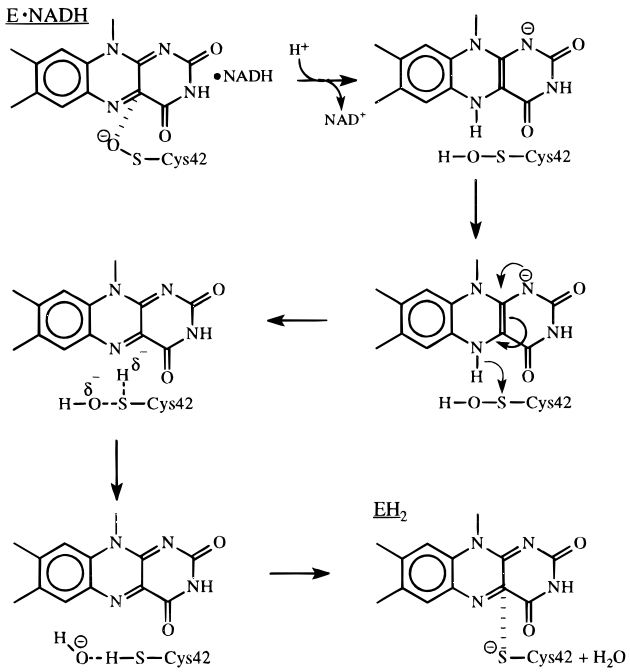

FIGURE 5: Schematic of the initial "priming" step which generates the thiolate form of Cys42 required for the EH_2 charge-transfer interaction. Hydride transfer from FAD-N(5) to Cys42-Sγ yields the oxidized FAD while reducing the Cys42-SOH to Cys42-SH and eliminating OH^-. Proton abstraction by the leaving group OH^- yields the product H_2O and generates the thiolate form of Cys42.

hydride acceptor. In oxidized GR (Karplus & Schulz, 1989), FAD-C4A is in line with the Cys58−Cys63 disulfide, optimizing the orientation for an S_N2 displacement on Cys63-Sγ by FAD-C4A (interatomic distance = 3.5 Å). In the peroxidase, however, the Cys42-Sγ−O bond is more nearly parallel to the plane of the flavin, and the FAD-C4A:Cys42-Sγ distance of 3.70 Å is less favorable for such a nucleophilic displacement. Direct hydride transfer from FAD-N5 to Cys42-Sγ is an alternative, but the interatomic distance in our model is 4.0 Å. Reduction of the peroxidase appears to be rate-limiting over the pH range (Crane et al., 1995), and the decrease of k_{cat} above pH 6.5 is consistent with the requirement for a proton in reduction. If, as suggested, Cys42-SOH is stabilized as the sulfenate anion, protonation will be required prior to elimination of OH^- by either the nucleophilic displacement or hydride-transfer mechanisms of Cys42-SOH reduction. Recent work has shown that His10 is not an essential acid−base catalyst in the peroxidase (Crane et al., 1996), but we have also shown that the protein stabilizes the N(1)-anionic form of $FADH_2$ on reduction (Poole & Claiborne, 1989b). Given the close approach of 3.3 Å between the FAD-N1 and the sulfenate oxygen, it seems likely that hydride transfer to FAD, introducing a negative charge in the N(1)−C(2)═O(2α) region, would be likely to follow protonation of the sulfenate anion (Figure 5). Hydride transfer to Cys42-Sγ from FAD-N(5) yields the oxidized FAD while reducing the Cys42-SOH to Cys42-SH (the proton now on Cys42-SH originates with the hydride ion) and eliminating OH^-. The pK_a of Cys42-SH is ≤4.5 (Poole & Claiborne, 1986); proton abstraction by the leaving group OH^- yields the product H_2O and generates the thiolate form of Cys42 required for the EH_2 charge-transfer interaction. During the reduction of GR, Cys63-Sγ undergoes a net approach of 0.2 Å toward the FAD pteridine moiety in establishing the EH_2 charge-transfer interaction (Karplus &

Schulz, 1989). A similar movement of Cys42-Sγ in the peroxidase toward FAD-C4A would stabilize the thiolate approximately 3.5 Å from the C4A position. The structure of the peroxidase EH_2 form will be required to test this proposal and to determine those factors involved in Cys42-thiolate stabilization.

The native Cys42-SOH structure of NPX can be compared with the non-native Cys42-SOH structures reported for the rat trypsin S195C mutant (Wilke et al., 1991), the subtilisin mutants 8397 and 8397+1 (Kidd et al., 1996), and the HIV-1 protease complex with the inhibitor U-75875 (Thanki et al., 1992). An X-ray structure has also been reported for the unexpectedly stable 4,6-dimethoxy-1,3,5-triazine-2-sulfenic acid (Tripolt et al., 1993). The only reports of other naturally occurring, functional Cys-SOH residues at present are found in the redox-regulated DNA-binding proteins Fos and Jun (Abate et al., 1990), OxyR (Storz et al., 1990; Kullik et al., 1995), BPV-1 E2 protein (McBride et al., 1992), and nuclear factor I (Bandyopadhyay & Gronostajski, 1994). Kullik et al. (1995) have recently suggested that Cys199 represents the regulatory redox center of OxyR, undergoing reversible oxidation by H_2O_2 to Cys-SOH as an obligatory step in transcriptional activation. Bandyopadhyay and Gronostajski (1994) have identified a conserved cysteine (Cys3) in the nuclear factor I family of DNA-binding proteins, which is sensitive to reversible oxidation *in vitro*, and have suggested that a Cys-SOH form may be responsible for the inhibition of DNA binding. Similar evidence has been considered in the suggestion that Fos-Cys154 and Jun-Cys272 may be oxidized to Cys-SOH, inhibiting their respective DNA-binding activities, and a Cys-SOH form of Cys340 in the BPV-1 E2 protein has been proposed to cause the reversible inactivation of DNA binding as well (McBride et al., 1992). Hegde et al. (1992) have reported the X-ray crystal structure of the complex between the BPV-1 E2 DNA-binding domain and its DNA target, and Cys340 has been identified as one of four conserved residues from the "recognition" helix which interact directly with "identity" elements of the DNA. Specifically, Cys340-Sγ donates a hydrogen bond to the O6 oxygen of a guanine base, while simultaneously accepting a hydrogen bond from the 6-amino group of an adenine located in the adjacent base pairing. Reversible oxidation of Cys340 to the Cys340-SOH could easily interfere with this protein−DNA interaction and lead to diminished DNA-binding activity.

Our structural determination of a functional cysteine-sulfenic acid in a protein molecule indicates that these redox-active moieties represent an emerging and important new class of redox centers utilized in biological reactions.

REFERENCES

Abate, C., Patel, L., Rauscher, F. J., III, & Curran, T. (1990) *Science 249*, 1157−1161.

Allison, W. S. (1976) *Acc. Chem. Res. 9*, 293−299.

Bandyopadhyay, S., & Gronostajski, R. M. (1994) *J. Biol. Chem. 269*, 29949−29955.

Brünger, A. (1992) *XPLOR 3.0: A System for Crystallography and NMR*, Yale University, New Haven, CT.

Claiborne, A., Miller, H., Parsonage, D., & Ross, R. P. (1993) *FASEB J. 7*, 1483−1490.

Claiborne, A., Ross, R. P., Ward, D., Parsonage, D., & Crane, E. J., III (1994) in *Flavins and Flavoproteins 1993* (Yagi, K., Ed.) pp 587−596, de Gruyter, New York.

Crane, E. J., III, Parsonage, D., Poole, L. B., & Claiborne, A. (1995) *Biochemistry 34*, 14114−14124.

Crane, E. J., III, Parsonage, D., & Claiborne, A. (1996) *Biochemistry 35*, 2380−2387.

Fox, K. M., & Karplus, P. A. (1994) *Structure 2*, 1089−1105.

Hegde, R. S., Grossman, S. R., Laimins, L. A., & Sigler, P. B. (1992) *Nature 359*, 505−512.

Hogg, D. R. (1990) in *The Chemistry of Sulphenic Acids and Their Derivatives* (Patai, S., Ed.) pp 361−402, John Wiley & Sons, New York.

Karplus, P. A., & Schulz, G. E. (1989) *J. Mol. Biol. 210*, 163−180.

Karplus, P. A., Fox, K. M., & Massey, V. (1995) *FASEB J. 9*, 1518−1526.

Kice, J. L. (1980) *Adv. Phys. Org. Chem. 17*, 65−181.

Kidd, R. D., Yennawar, H. P., Sears, P., Wong, C.-H., & Farber, G. K. (1996) *J. Am. Chem. Soc. 118*, 1645−1650.

Kim, S.-H., Quigley, G. J., Suddath, F. L., McPherson, A., Sneden, A., Kim, J. J., Weinzierl, J., & Rich, A. (1973) *J. Mol. Biol. 75*, 421−428.

Kullik, I., Toledano, M. B., Tartaglia, L. A., & Storz, G. (1995) *J. Bacteriol. 177*, 1275−1284.

Lawkowski, R. A., MacArthur, M. W., Moss, D. S., & Thornton, J. M. (1992) *J. Appl. Crystallogr. 26*, 283−291.

Liu, T.-Y. (1977) in *The Proteins* (Neurath, H., & Hill, R. L., Eds.) 3rd ed., Vol. 3, pp 239−402, Academic Press, New York.

Mande, S. S., Parsonage, D., Claiborne, A., & Hol, W. G. J. (1995) *Biochemistry 34*, 6985−6992.

McBride, A. A., Klausner, R. D., & Howley, P. M. (1992) *Proc. Natl. Acad. Sci. U.S.A. 89*, 7531−7535.

Miller, H., Mande, S. S., Parsonage, D., Sarfaty, S. H., Hol, W. G. J., & Claiborne, A. (1995) *Biochemistry 34*, 5180−5190.

Navaza, J. (1994) *Acta Crystallogr. A50*, 157−163.

Otwinowski, Z. (1993) in *Proceedings of the CCP4 Study Weekend: Data Collection and Processing* (Sawyer, L., Issacs, N., & Bailey, S., Eds.) pp 56−62, SERC Daresbury Laboratory, England.

Parsonage, D., & Claiborne, A. (1995) *Biochemistry 34*, 435−441.

Parsonage, D., Miller, H., Ross, R. P., & Claiborne, A. (1993) *J. Biol. Chem. 268*, 3167−3167.

Poole, L. B., & Claiborne, A. (1986) *J. Biol. Chem. 261*, 14525−14533.

Poole, L. B., & Claiborne, A. (1988) *Biochem. Biophys. Res. Commun. 153*, 261−266.

Poole, L. B., & Claiborne, A. (1989a) *J. Biol. Chem. 264*, 12330−12338.

Poole, L. B., & Claiborne, A. (1989b) *J. Biol. Chem. 264*, 12322−12329.

Read, R. J. (1986) *Acta Crystallogr. A42*, 140−149.

Ross, R. P., & Claiborne, A. (1991) *J. Mol. Biol. 221*, 857−871.

Stehle, T., Ahmed, S. A., Claiborne, A., & Schulz, G. E. (1991) *J. Mol. Biol. 221*, 1325−1344.

Stehle, T., Claiborne, A., & Schulz, G. E. (1993) *Eur. J. Biochem. 211*, 221−226.

Storz, G., Tartaglia, L. A., & Ames, B. N. (1990) *Science 248*, 189−194.

Thanki, N., Rao, J. K. M., Foundling, S. I., Howe, W. J., Moon, J. B., Hui, J. O., Tomasselli, A. G., Heinrikson, R. L., Thaisrivongs, S., & Wlodawer, A. (1992) *Protein Sci. 1*, 1061−1072.

Tripolt, R., Belaj, F., & Nachbaur, E. (1993) *Z. Naturforsch. 48B*, 1212−1222.

Wilke, M. E., Higaki, J. N., Craik, C. S., & Fletterick, R. J. (1991) *J. Mol. Biol. 219*, 511−523.

Williams, C. H., Jr. (1992) in *Chemistry and Biochemistry of Flavoenzymes* (Müller, F., Ed.) Vol. III, pp 121−211, CRC Press, Boca Raton, FL.

BI961037S